Journal of Theoretical and Applied Information Technology
15th May 2026. Vol.104. No.9

ISSN: 1992-8645 www.jatit.org E-ISSN: 1817-3195

ENHANCING RELIABILITY AND DATA RATE IN MOLECULAR COMMUNICATION FOR IOBNT USING MOLCOMMLSTM

OMAR KHALID SALIH ALHAFIDH[1] , MAWADA MUHAMMAD SULIMAN [2] , SADOON HUSSEIN ABDULLAH[3] , SOHA MOHAMED HASSAN[4]

[1]Associate Lecturer, College of Education for Human Sciences, Mosul University, Mosul, Iraq

[2] Lecturer. Department of Chemistry, Collage of Science, Mosul University, Mosul, Iraq

[3]PhD in Computer Science, Associate Professor. Department of Physics, Collage of Science, Mosul University, Mosul, Iraq

[4]Associate Lecturer, School of Computer Science and Technology, Harbin Institute of Technology, China

E-mail: [1]omaralhafidh@uomosul.edu.iq, [2]Mwada.m.suliman@uomosul.edu.iq, [3]Sadosbio113@uompsul.edu.iq, [4]Sc.soha@yahoo.com

ABSTRACT

Molecular communication (MC) in bio-nano things (IoBNT) is one of the promising paradigm for nanoscale networks, where information is encoded in the concentration of molecules. However, reliability in the MC system and data rate mapping remain challenges in achieving high efficiency and accurate symbol detection during communication between transceivers. In order to solve these challenges, a novel approach called MolCommLSTM is proposed, which combines an adaptive modulation technique and a deep long-short-term memory (LSTM) detector for symbol detection. The proposed MolCommLSTM system model dynamically adjusts molecular concentration levels based on the estimated distance between the transmitter (TN) and receiver (RN) nano-machines to optimize system performance. In addition, a deep LSTM directly maps the received signals to the transmitted symbols, facilitating efficient and accurate symbol detection. For theoretical comparison, a traditional detection algorithm called the maximum likelihood detector (MLE) is used. The MLE is implemented as a threshold-based decision rule where the detected signal strength is compared against a predefined threshold to infer the transmitted symbol. This approach efficiently demodulates the original signal by identifying the slot with the highest likelihood of a reaction, corresponding to the highest concentration of molecules. Extensive experimental results show that the proposed MolCommLSTM system model significantly improves the symbol error rate (SER) and achievable data rate (ADR) over the concentration position shift keying (CPSK) modulation scheme. Furthermore, the proposed MolCommLSTM system model effectively addresses the bias effect and minimizes inter-symbol interference (ISI) in the diffusion based molecular channel, resulting in superior performance compared to the MLE detector.
Keywords: *Reliability, Data Rate, Communication, IOBNT, MOLCOMMLSTM*

1. INTRODUCTION

The IoBNT is a breakthrough in future technologies that can bring changes to nano-communication [1]. The nano communication systems can be linked to each other and then onto an external computing part, e.g., cloud and edge computing. While IoBNT is an artificial biology that creates the cells in a way that allows them to have features like devices for the traditional Internet of Things (IoT) [2]. Because IoBNT systems are based on molecular communication (MC), which leverages the features of molecules for information exchange and has been recognized as one of the most popular IoBNT methods due to their biocompatibility, energy efficiency, and ubiquity in nature [3]. MC has emerged as a promising communication paradigm for bio-nanoscale networks, offering unique opportunities for information exchange at the molecular level [4]. Unlike conventional wireless communication, MC leverages the concentration of biomolecules to encode and transmit data between nano machines [5]. MC draws inspiration from the natural

processes that occur within biological systems, where cells communicate with each other using signaling molecules [6]. Furthermore, molecular communication (MC) has distinct benefits in nanoscale networks, where traditional electromagnetic approaches are constrained by size and energy [7].MC has high promise in biomedical sensing, environmental monitoring, targeted drug delivery (TDD), nanomedicine, and IoBNT [8].

MC, like classical electromagnetic (EM) communication, is characterized as wired or wireless. ICT researchers define MC into three ranges: short-range (nanometer scale), mid-range (micrometer to centimeter), and long-range (centimeter to meter)[9]. Short-range MC, also known as molecular nano-communication, uses breakthroughs in biology and nanotechnology to build functioning nanoscale devices, or nano-machines. Basic communication units consist of a transmitter nanomachine (TN) and a receiver nanomachine (RN) [10]. When numerous nanomachines interact together, they build nanonetworks, which connect nanoscale MC to macroscale EM communication and the internet [11].

MC is a new communication paradigm with enormous promise from the standpoint of communication engineering. This new technology uses molecules as information carriers to allow communication between nanoscale devices. Despite its intriguing possibilities, MC is still in its early stages, and creating a full MC system faces several problems. One of these issues is to devise an efficient modulation strategy for encoding information onto information-carrying particles. Another critical component is developing strong ways to correctly detect and decode information from diffused signals.

In MC, CSK is a modulation technique that uses the number of released molecules to encode information [12][13], which unfortunately suffers from ISI due to residual molecules interfering with the detection of the current symbol [14][15][16]. CPSK avoids ISI by carrying information over the position of the molecules, similar to PPM in EM communication [17] [18]; it is a fixed modulation scheme, however, without the ability to adapt to dynamic channel conditions.MC channels vary due to the TN–RN distance, molecule concentration fluctuations, interfering substances, and environmental changes. Traditional linear models are insufficient to capture the nonlinear dynamics of molecular signaling and chemical interactions.

To address such limitations, we present MolCommLSTM, an approach to adaptively modulate in relation to estimated TN-RN distance and channel conditions. The considered system models free diffusion-based MC channels [19, 20] and includes the ligand-receptor binding process (LRBP) [21-24]. LSTM networks decode the received signals to predict the transmitted symbols, which would provide a better decoding performance under complex conditions. For comparison, we consider an MLE that requires channel knowledge a priori [25-27]. In contrast, MolCommLSTM learns directly from the data. The results show that MolCommLSTM is effective in handling nonlinearities, improves symbol detection, and outperforms traditional MLE, thus ensuring a robust performance under the variations of MC channel conditions. Our main contributions are summarized as follows:

- We propose a novel MolCommLSTM transmitter that employs adaptive modulation, dynamically adjusting molecular concentration levels based on the estimated TN–RN distance. This approach mitigates channel variations and overcomes limitations of fixed schemes like CPSK, addressing challenges such as ISI, symbol error rate (SER), and achievable data rate (ADR).
- The MolCommLSTM receiver uses a deep LSTM architecture for symbol detection. It directly maps received signals to transmitted symbols using systematic training on input-output pairs. Inputs are derived from Ligand-Receptor Binding Process (LRBP) probability estimates, while outputs correspond to transmitted pulse positions.
- Through numerical simulations and performance evaluations, we demonstrate that combining adaptive modulation with deep LSTM-based detection provides a reliable, adaptive, and high-performance solution for nano-scale communication, consistently outperforming traditional MLE approaches.

2. RELATED WORKS

Many researchers have conducted deep learning (DL) studies in the domain of MC [28]–[33]. Lee et al. [28] used a deep learning method to create a model for the channel of a molecular multi-

input and multiple-output (MIMO) system. They explored the impact of adjusting the number of neural networks used in the modeling process. IN [29], researchers have introduced an approach using sliding bidirectional recurrent neural networks (BiRNN) for detection with the help of deep learning approaches. The authors have presented an automatic learning model system based on experimental data and executed data detection without using composite channel approximation or data equalization methods. In [30], the authors presented an ANN approach that uses raw data for the robust receiver schema. A study by O'Shea and Hoydis [31] has presented DL models for the physical layer of modeling communication systems, which are created by seeing the communication system as an auto encoder to optimize the receiver and transmitter components. Moreover, the principle of RTN (radio transformer networks) is used as a way to build competence in ML (machine learning) frameworks. The study also describes the CNN application for the classification of modulation in raw IQ samples to retain precision relative to conventional systems. Similarly, Qin et al, [32] studied DL for the development of communication schemes. The work discussed the current development of DL-based physical layer communication. Alshammri et al. [34] presented an adaptive threshold detection technique to demodulate processed data by off-key modulation, which united ANN with the fuzzy technique in MC through the diffusion environment. In [35], the authors applied the structure of the MC auto-encoder and jointly optimized the transceiver (transmitter and receiver) using Deep Reinforcement Learning (DRL). In [36], the authors studied deep neural networks (DNN), support vector regression (SVR), logistic regression (LR) and ridge regression (RG) to model the signal received for a spherical receiver and trapezoidal container of MC via a diffusion framework. In [37], a cooperative and time-varying bidirectional recurrent neural network (CTBRNN) is devised as a signal detection approach. Shrivastava et al. [38] presented a neural network capable of extracting features from the filtered signal to identify and detect unknown bits in MC. Kose et al. [39] investigated the possibility of using molecular signals and deep learning techniques to detect and locate a silent entity. Furthermore, in another study by different authors [40], a data-driven detection approach was proposed using DL algorithms to eliminate the dependency on channel impulse response for the model-based detector. Bai et al. [41] employed a convolutional network to detect signals in an MC system that utilizes bacteria as carriers of information. Vakilipoor, Fardad, et al, [42] presents an approach to detect transmitted symbols in a biological MC testbed using a hybrid deep learning algorithm. The algorithm comprises convolutional and recurrent neural network(RNN). Cheng, Zhen, et al, [43] introduced a signal detector for a mobile multi-user MC system, employing a Transformer based model. The detector enhances signal accuracy by training a Transformer-based model at different transmitter-receiver distances.

However, the performance and accuracy of symbol detection in MC systems with varying channel conditions cannot be matched by the methods mentioned above. The primary distinction between our research and previous studies is the modulation technique used in the MC system. In contrast to our approach, most existing research focuses on traditional modulation schemes such as concentration shift key (CSK), OOK modulation, and binary-concentration shift keying (BCSK). Inspired by the aforementioned issues, our work proposes an adaptive modulation-based MC model that adjusts molecular concentration levels based on the estimated distance between the TN and RN. Adaptive modulation can help reduce ISI and enhance transmission efficiency in the MC system. Another key difference between our approach and previous studies is the network architecture used for the detection of symbols based on DL. In contrast to previous studies that utilized multilayer perception,RNN and regression models for MC detection, our approach employs a deep LSTM architecture. Moreover, recent studies [44]-[46] have further emphasized the importance of data driven and adaptive approaches in MC. These works highlight the growing trend towards intelligent system. However they still primary focus on receiver side improvement without jointly optimizing transmitter and receiver. This limitation further motivates the need for the proposed approach.

3. PRINCIPLE OF CPSK MODULATION

CPSK is a modulation technique used in MC to encode information such as the position of molecular concentration [17]. CPSK is a modulation technique that combines two existing methods: concentration shift keying (CSK) [47] and pulse position modulation (PPM) [48]. In PPM, the information is encoded in the timing of the molecule release. CPSK combines both methods by using different concentration levels and different time slots to represent different symbols. CPSK can

transmit multiple bits of information within each symbol duration. the total transmitted time T_{tx} is divided into eight slots. Each slot represents the duration of transmission of one symbol (t_s). With 8-CPSK, three bits can be transmitted per symbol. This means that each symbol can represent one out of eight possible combinations of three bits (000 to 111). The total transmission time T_{tx} is given by

$$T_{tx} = M * t_s \quad (1)$$

Mathematically, the transmitted signal Q(t) from T N using CPSK modulation M-ary can be represented as follows [17]:

$$Q(t) = \begin{cases} Q_s & if(m-1)t_s \le t \le mt_s, \\ 0 & otherwise. \end{cases} \quad (2)$$

Here, $m \in \{1, 2, 3, 4, 5, \ldots, M\}$ represents the position of the pulse $(M = 8)$. Q_s represents the molecular concentration per symbol. Q_s is given by the following equation:

$$Q_s = log_2(M) * Q_b \quad (3)$$

where Q_b represents the molecular concentration required to transmit one bit of information. In figure 1, an example of the CPSK modulation for 8-ary CPSK, to transmit the signal 010 with $(t_s) = 5$ is shown below.

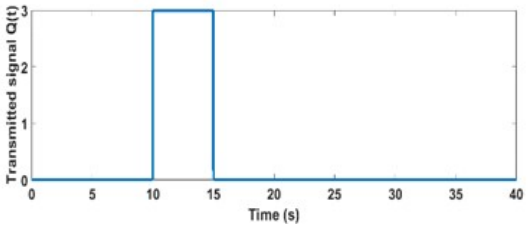

Figure 1: Transmitted signal "010" for M=8 at $(t_s) = 5$.

Using CPSK can increase the data rate and reduce the inter-symbol interference (ISI) compared to using CSK or PPM alone. However, CPSK also has some challenges and limitations, such as:

- The receiver needs to estimate both the concentration and the position of the received signal, which may introduce errors or complexity.
- The transmitter needs to adjust the concentration levels and the time slots according to the channel conditions, such as distance, noise, and interference.

To compensate for the drawbacks of CPSK, we propose a new adaptive modulation algorithm. In this algorithm, TN adapts the concentration level for each symbol based on an estimate of the distance to the RN

3. MOLCOMMLSTM SYSTEM METHODOLOGY

4.1 System Model Formulation

When numbering equations, enclose numbers in parentheses and place flush with right-hand margin of the column. Equations must be typed, not inserted.

As shown in Figure 2, this work considers a diffusion-based MC system composed of two nano-machines, a nano-transmitter (TN) and a nano-receiver (RN). The medium through which molecules propagate is a free diffusion channel in the air [49] [50]. This indicates that the molecules freely diffuse through the air without significant barriers or restrictions. In TN, information is encoded on the basis of the positon concentration of the molecular. The TN then uses an adaptive modulation-based CPSK. In adaptive CPSK modulation, we adjust concentration level according to the distance between the TN and RN. For example, we increase the concentration level for each symbol as the distance between the TN and RN increases to overcome the decrease in the concentration level at the RN. After that, the modulated molecular signals are released into the air by the TN. The molecular signals travel through the air as they diffuse and eventually reach the RN. In the RN, molecules are received and processed using a mechanism called the Ligand-Receptor Binding Process (LRBP). In this process, specific receptors on the RN selectively bind to the molecules transmitted on the basis of their position. Using the information obtained from the LRBP, the RN can decode the bits of transmitted data. Since the modulation scheme used is adaptive CPSK, the RN can determine the positions at which the molecules were modulated. Because of the LRBP mechanism, some molecules may not be bound by the ligand and remain in the channel. We demodulate the data by selecting the maximum probability value as the proper received symbol position. MLE is used as a detector on the RN side. Moreover, deep LSTM is applied to improve symbol detection at RN.

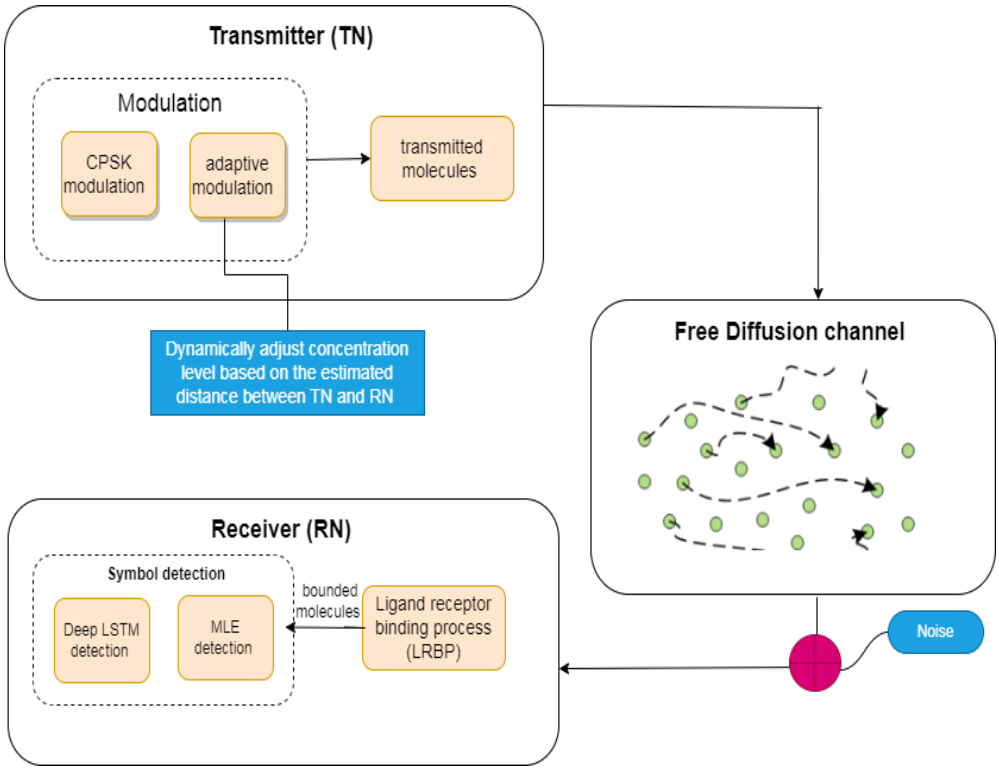

Figure 2 A visual representation framework of the proposed MolCommLSTM system model approach.

4.2 Proposed Adaptive Modulation

In our system, we propose an adaptive modulation scheme for MC, where the symbol concentration level is adjusted based on the distance between TN and RN. The algorithm adapts to changes in distance and concentration level. It involves estimating distance d to the RN, selecting the appropriate set of the concentration level based on d, mapping data to symbols, releasing molecules at the beginning of each symbol duration according to the selected concentration level. This ensures that the RN can accurately detect transmitted symbols even when there are changes in distance and concentration level between TN and RN. Moreover, this can help improve the reliability of the system.

Algorithm 1 presents the detailed procedure of the proposed adaptive modulation.

Algorithm 1: Proposed adaptive modulation

Require: Number of symbols(M), symbol duration (t_s), total transmission time (T_{tx}), molecular concentration per bit (Q_b), distance between the TN and RN, (d), pulse position(m).

Ensure: Selected molecular concentration levels (Q_s) based on the estimated distance.

Initialize the matrix $Q_{s\,sel}$ of size

M × 2 to store molecular concentration levels Q_s= new matrix(M,2).

Compute molecular concentration levels for different distances and store them in Qs.

for $i \leftarrow 1$ *to* M **do**

if $d_{hat} \leq 5$ **then**

$Q_s[i][1] = log_2(M) * Q_b * i$

end if

if $d_{hat} \geq 5$ **then**

$Q_s[i][2] = log_2(M) * Q_b * 2 * i$

end if

end for

Estimate the distance to the receiver $\triangleright d_{hat}$ = d // Assume perfect distance estimation

Select molecular concentration levels based on the estimated distance.

if $d_{hat} \leq 5$ **then**

$Q_{s\,sel} = Q_s\,[:, 1] \triangleright$ Set $Q_{s\,sel}$ to the first column of Q_s

else if $d_{hat} \geq 5$ **then**

$Q_{s\,sel} = Q_s\,[:, 2] \triangleright$ set $Q_{s\,sel}$ to the second column of Q_s

end if

return $Q_{s\,sel} \triangleright$ // Return $Q_{s\,sel}$ as the output

if $(m-1)t_s \leq t \leq mt_s$ *then* $Q(t) \leftarrow Q_{s\,sel}$

else

$Q(t) \leftarrow 0$

end if

End

a) Channel Communication: In this paper, we investigate a diffusion-based MC channel.

It leverages quantum or particle theory propagation to model molecular propagation, in contrast to conventional electromagnetic (EM) wave propagation. The channel quantum response (CQR) is developed as an analogous concept to the time-varying channel impulse response (CIR) encountered in conventional EM communication. Based on the work presented in [47], we have adapted the behavior of molecular propagation in a free diffusion environment, such as air. The mathematical representation of the MC channel's impulse response, denoted as $C(d,t)$ is expressed as follows:

$$C(d,t) = \frac{1}{(4\pi Dt)^{\frac{3}{2}}} e^{-\frac{d^2}{4Dt}} \quad (4)$$

where D corresponds to the diffusion coefficient of the MC channel, and d represent the distance between (TN) and the (RN) in cm. In Figure 3, the channel impulse response $C(d,t)$ is shown that varies with the d between TN and RN. We can see that as d increases, the magnitude of CQR becomes less (which means that few molecules reach RN). After diffuse through the channel, the arrived signal at the RN can be given as

$$U(d,t) = Q(t) * C(d,t) \quad (5)$$

where, $(*)$ refers to the convolution operation.

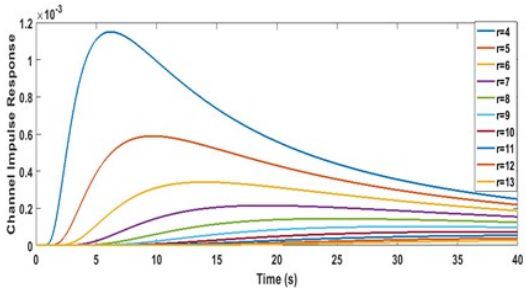

Figure 3 channel $C(d,t)$ *according to* d *with* t_s*= 5 sec and* $D = 0.43\ cm^2 s^{-1}$.

b) Reception Process: We consider the ligand-receptor binding(LRBP) process in the proposed system model. Once the TN reaches to RN through the free diffusion channel, the transmitted molecules encounter the receptors, referred to as ligand molecules. This interaction causes a chemical reaction that results in a short pulse known as LRBP. Some molecules persist in the medium because they do not collide with receptors, resulting in ISI. The RN decodes symbols by measuring concentrations in each time slot using its receptors. A propensity function determines the average frequency of ligand-receptor interactions over a certain time interval, simulating LRBP receipt and considering incoming molecules as a random variable in the signal-and-noise model. Given the high number of diffusing molecules, monitoring each individually is impracticable, hence the propensity function [24] is defined as:

$$a(U(d,t)) = \eta P = \eta(RU(d,t)) = \eta RU(d,t) \quad (6)$$

Here, η represents the probability rate constant specific to molecular reactions between a ligand molecule and a receptor, while R corresponds to the concentration of receptors on the RN. We can calculate $P = RU(d,t)$, where $U(d,t)$ is defined by equation (5). Because the precise solution to the propensity function in the Continuous-Time MC process is difficult due to its intrinsic unpredictability, we use an approximation technique using the following constraints. Firstly, we assume that the time interval dt is very small, leading to

$$a(U(d,t)) \approx a(U(d,t')), for\ all\ t' \in [t, t + dt]$$

This assumption implies that reactions occurring within $[t, t + dt]$ are independent of each other. Consequently, the number of reactions within the following time interval $[t, t + dt]$ adheres to a statistically independent Poisson's random variable with a rate of $\lambda = a(U(r,t))dt$. Secondly, we assume that dt is large, leading to a significantly larger number of reactions $(\gg 1)$ within $[t, t + dt]$. Under these conditions, the previously mentioned Poisson random variable can be approximated by a normally distributed random variable with the same mean and variance, represented as, denoted as $N \sim (\lambda, \lambda)$. In our system, the release of molecules can occur at any point within the symbol intervals during the total transmission time. Thus, the probability of ligand-receptor reaction during the interval $[(i-1)t_s, it_s]$ can be revealed as a randomly distributed variable $N_j \sim N(\mu_i, \sigma_i^2)$, where μ_i represents the mean and σ_i^2 is the variance. These values are given by:

$$\mu_i = \sigma_i^2 \int_{(i-1)t_s}^{it_s} a\big(U(d,t)\big)dt \quad (7)$$

where $i \in \{1, 2, \ldots, M\}$. We employ this method to evaluate the likelihood of a reaction occurring

during each time interval of t_s using the LRBP. To recover the original signal, we apply the Maximum Likelihood Estimation (MLE) function. In this context, the MLE is implemented as a threshold-based decision rule derived from the MLE principle, where the detected signal strength N_j is compared against a predefined threshold to infer the transmitted symbol [51][52]. The threshold is set to half the molecular concentration per symbol, $\xi = \frac{Q_s}{2}$, simplifying the decision-making process while retaining the accuracy of MLE detection:

$$\hat{m} = \begin{cases} 1 \; if \; N_j \geq \xi \\ 0 \; otherwise \end{cases} \quad (8)$$

This threshold-based technique demodulates the signal by choosing the slot with the greatest possibility of a reaction, which corresponds to the peak molecule concentration. By combining these approximations with the MLE-based threshold, the system can consistently infer transmitted symbols, providing an effective and computationally economical demodulation technique for MC systems.

4.3 Deep LSTM for Symbol Detection

In this section, we describe a deep-learning-based receiver design for the MC system. Because the symbols are broadcast in different time intervals, the dataset is time-series in nature. To capture these temporal patterns, we employ an LSTM network, a form of recurrent neural network that is ideally adapted to learning long-term dependencies. The LSTM also makes classification judgments by using prior inputs and outputs. In the next section, we compare the performance of this LSTM-based receiver to that of the typical MLE receiver.

a) Data generation: The generation of input and output data is critical for modeling and training the MC system. In this subsection, we will go into the details of how input and output data are generated and collected for subsequent analysis and training. To assess the performance of the system and train a DL model, we performed multiple trials, iterating over different distances between the transmitter and receiver. The core idea is to train the receiver using input-output data pairs, with input values derived from the probability estimates obtained through the LRBP. This training process's output data is set to the matching transmitted pulse positions. Figure 4 depicts the process of creating a training data set.

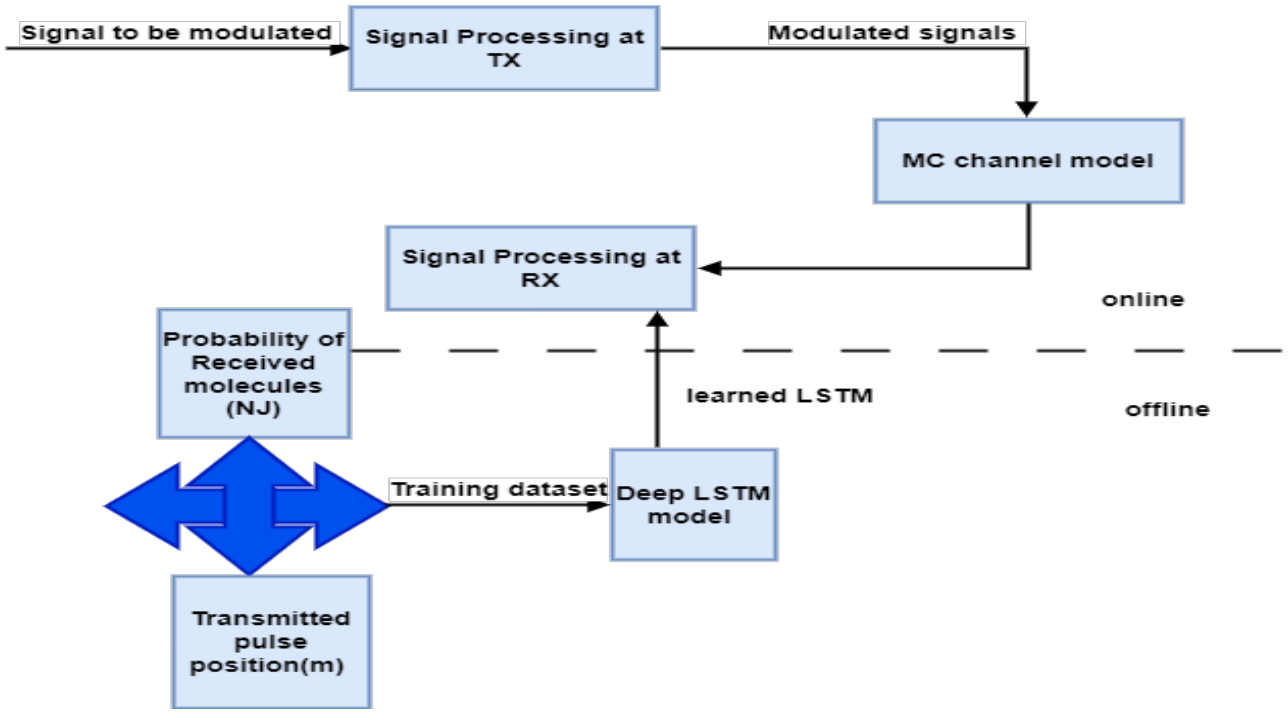

Figure 4 Generation of the training data set for deep LSTM training process.

b) Deep LSTM model architecture: LSTM is a deep neural network that can handle time-varying input and develop long-term relationships among sequences [53]. In this paper, we utilize Keras to create an LSTM model specifically for the MC system in IoBNT. The architecture consists of two LSTM layers with 256 units each. The first layer returns sequences, followed by dropout (0.2) and layer normalization to prevent overfitting and stabilize training. Dense layers with Leaky ReLU activation further refine the features, whereas the output layer employs softmax for multi-class scenarios or sigmoid when M = 2. This approach allows for good symbol pattern learning and dependable prediction in the MC channel.

5. IMULATION RESULTS AND ANALYSIS

Following the introduction of the parameter settings, this section will proceed to show the results of our simulations based on the parameter settings shown in Table 1 of the values of the MC setting used in this study.

Table 1: MC system parameter values Table

Parameter	Value
Symbol duration(t_s)	(5,10,20,30)sec
Distance(d)	1:10cm
Diffusion Coefficient(D)	0.43
Modulation order (M)	2,4,8

5.1 Performance Analysis of Our Proposed Adaptive Modulation Based on MLE

In this section, we present the performance analysis of our proposed adaptive M-ary CPSK modulation for MC system. We evaluate the SER and the DR to assess the effectiveness of our approach. SER is a vital metric for assessing the dependability of MC systems since it measures the likelihood of wrongly decoding a symbol owing to noise and interference in the diffusion channel. Extensive simulations were conducted to assess the SER of our proposed technique at various distances and symbol lengths (t_s). Figures 5, 6, and 7 depict the SER curves for the MolCommLSTM model with adaptive modulation in 8-, 4-, and 2-ary schemes. The charts show how SER varies with distance for various t_s values. Adaptive modulation allows the system to change the modulation order based on channel circumstances, which improves reliability and spectral efficiency. The (8, 4, 2) arrangement implies that the system may transition between several modulation levels, allowing for flexibility in a variety of channel situations.

Each curve in Figures 5-7 corresponds to a distinct combination of distance and symbol duration, providing insight into how system performance varies with different conditions. This research refines and optimizes the suggested communication technique, ensuring its flexibility and resilience in real-world MC circumstances.

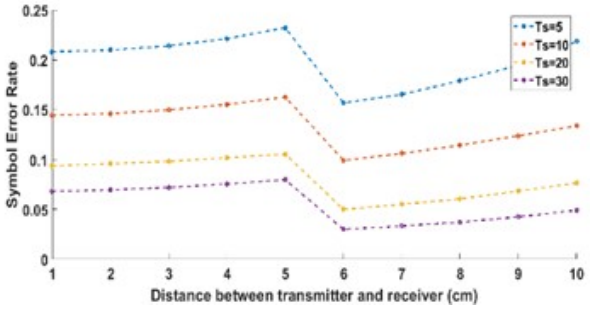

Figure 5 SER vs distance for different (t_s) of our proposed adaptive modulation where M=8.

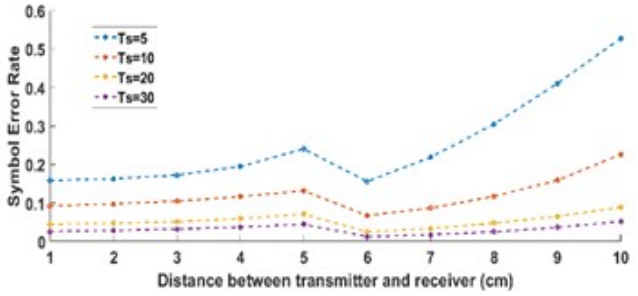

Figure 6 SER vs distance for different(t_s) of our proposed adaptive modulation where M=4.

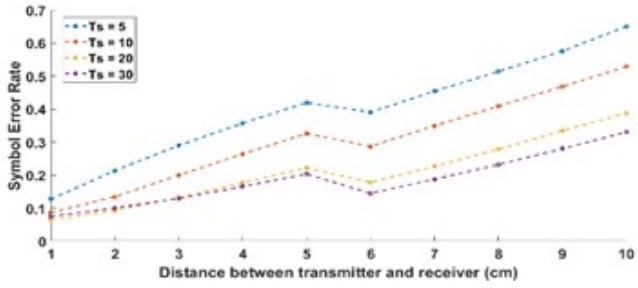

Figure 7 SER vs distance for different(t_s) of our proposed adaptive modulation where M=2.

Even the SER depends on several factors, such as the distance between the TN and RN, the concentration level of the transmitter, the diffusion coefficient of the molecules, the noise level of the channel, and the symbol duration (ts). The distance between TN and RN affects the SER because it determines how much the molecules diffuse before reaching the receiver. The longer the distance, the more the molecules spread out and lose their concentration, making it harder for the receiver to distinguish between different symbols. The previous results show that the SER increases as the distance increases for all values of d. However, the duration of the symbol (t_s) affects the SER because it determines how long the transmitter releases molecules per symbol and how long the receiver measures them. The longer t_s, the more molecules are released and measured, making it easier for the receiver to decode them. However, a longer t_s also reduces the data rate and increases the delay of MC. The proposed technique uses a fixed (t_s) values for all distances, which is chosen to balance between SER performance and data rate efficiency. The results show that this choice of t_s can achieve a low SER for all distances. we also can note that, when (t_s) increase SER decrease. We also can notice that, while decrease modulation order (M), decrease symbol error rate increase. The concentration level of the transmitter affects the SER because it determines how many molecules are released per symbol. The higher the concentration level, the more molecules are available for transmission, making it easier for the receiver to detect them.

However, a higher concentration level also increases the energy consumption and interference of MC. The proposed technique adapts the concentration level according to the distance and concentration level, using lower concentration levels for shorter distances, and higher concentration levels for longer distances. The results show that this adaptation can reduce the SER especially for long distance.

5.2 Achievable Data Rate (DR) Performance

The DR is another crucial metric for evaluating the efficiency of a communication system. It represents the maximum data rate that can be reliably transmitted over the diffusion based MC channel. Figures 8,9 show the MLE DR performance curves for our method using (8,4,2)-ary adaptive modulation over a range of distances values for fixed (t_s) value and different T_{tx}.

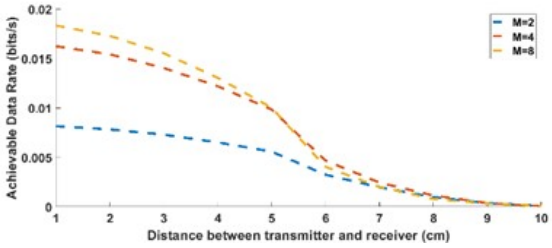

Figure 8 MLE DR vs distance for different M of our proposed adaptive modulation where T_{tx}=60.

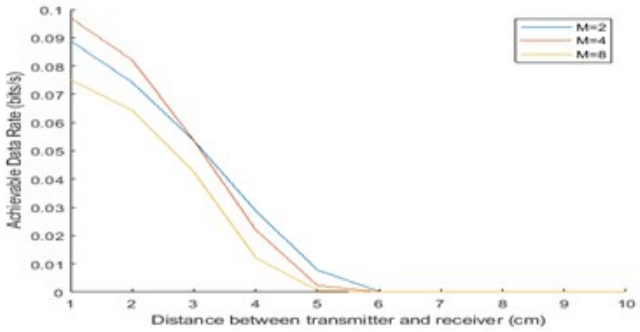

Figure 9 MLE DR vs distance for different M of our proposed adaptive modulation where T_{tx}=40.

from the results shown above in figure (8,9) we can notice that, higher modulation order (M), increase the DR.

5.3 Comparison With Fixed M-ary CPSK Modulation

To further validate the performance of our proposed adaptive modulation, we compared it with fixed modulation as shown in figure10 below. The proposed technique aims to improve the SER of the MC system by adapting the concentration level according to the distance between the TN and RN. The findings show that the suggested approach consistently delivers a lower SER than the fixed CPSK system, which uses a single concentration level across all symbols.

Across all tested distances, the suggested technique had a lower SER than CPSK. This demonstrates its potential to harness spatial variety and plasticity in molecular communication. Furthermore, by applying lower concentration levels across shorter distances, the approach reduces energy consumption and interference. Overall, the suggested technique provides robust SER performance and greater attainable data rates, making it a potential choice for dependable and efficient MC systems.

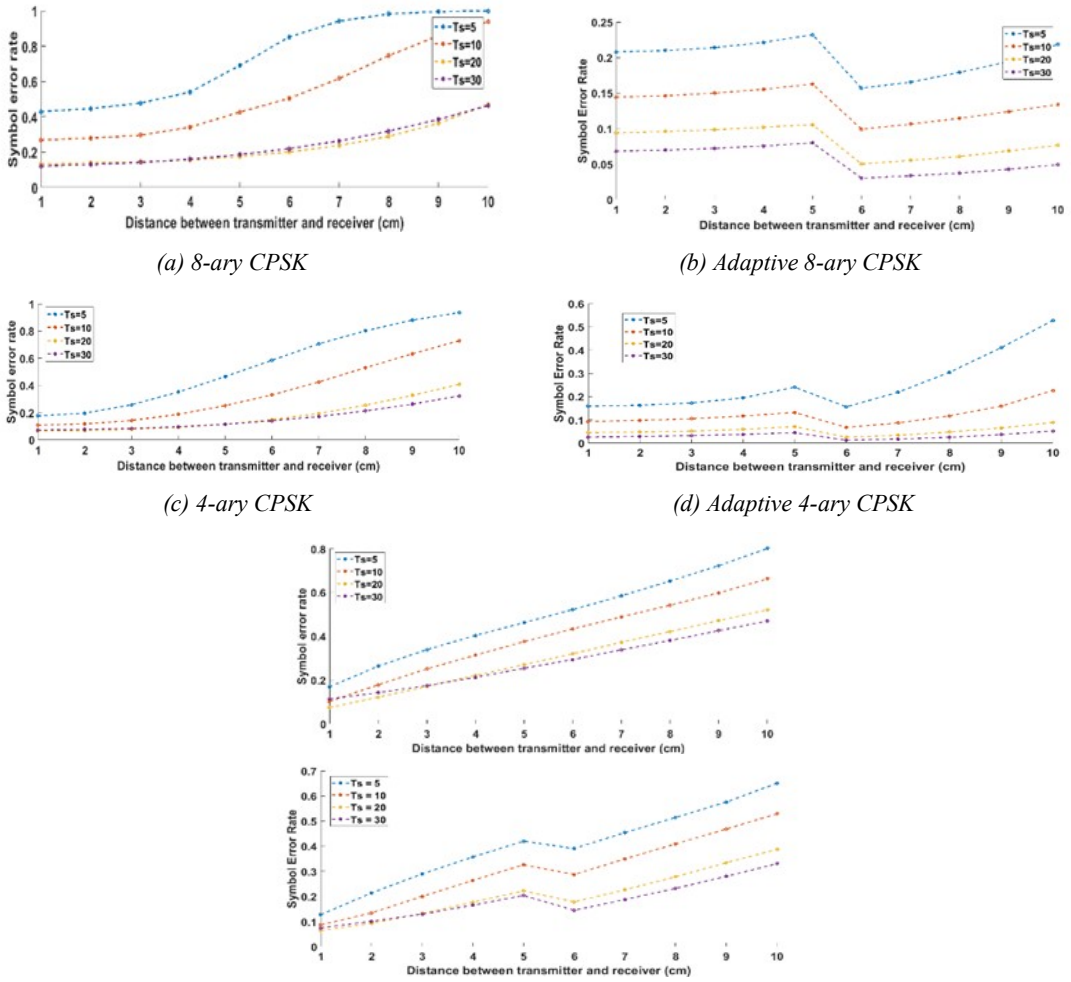

(a) 8-ary CPSK *(b) Adaptive 8-ary CPSK*

(c) 4-ary CPSK *(d) Adaptive 4-ary CPSK*

(e) 2-ary CPSK *(f) Adaptive 2-ary CPSK*

Figure 10 MLE SER comparison between fixed and our proposed adaptive modulation.

5.4 Training Results of MolCommLSTM for Symbol Detection

In this section, we investigate closely the training results and performance evaluation of deep LSTM for symbol detection in our System Method. In this study, we present an in-depth analysis of our deep LSTM-based symbol detection approach, highlighting the training process, performance metrics.

a) Training of the deep LSTM model: The propose model is instantiated with a diverse array of distinct configurations, in which the Adams optimizer is employed as a gradient descent-based optimization. We used the categorical cross entropy loss function, which shows the difference between the predicted and actual symbol labels. SER is the ratio of the number of misclassified symbols to the total number of symbols. The performance evaluation metric accuracy, which is based on the proportion of correctly detected symbols in the training and testing data sets, is a performance assessment. The Proposed model is trained using a subset of the provided data. Specifically, the training data set is split into training and validation sets, with a portion (20%) reserved for validation to monitor training progress. The proposed model undergoes training for a fixed number of 100 epochs with a batch size of 256. After training, the proposed model performance is evaluated on a separate test data set.

b) MolCommLSTM demodulation training results: in this section, curves of accuracy and loss, with respect to the number of epochs, for M=8,4,2 are presented. for the training we generated combined data for different distance values from 1 to 10 at different t_s values. In Figure 11, the training demodulation loss for M=8,4,2 are shown. The loss function calculates the error between the model's predictions and the

Journal of Theoretical and Applied Information Technology
15th May 2026. Vol.104. No.9

ISSN: 1992-8645 www.jatit.org E-ISSN: 1817-3195

actual target values at each epoch. Figure.11a, 11b, 11c plot the demodulation loss rate at training epochs = 100 for M=8,4,2 respectively. The loss rate decreases as the model goes through more epochs, which means that the model updates its parameters and gets better at predict accurately. The decrease of the loss rate over epochs indicates how the model learns and improves its demodulation performance. The general decrease of the loss rate over epochs indicates how the LSTM model learns and improves its demodulation performance on this data for different values of M. The exact shape and slope of the loss decrease provides insight into model convergence and learning rates.

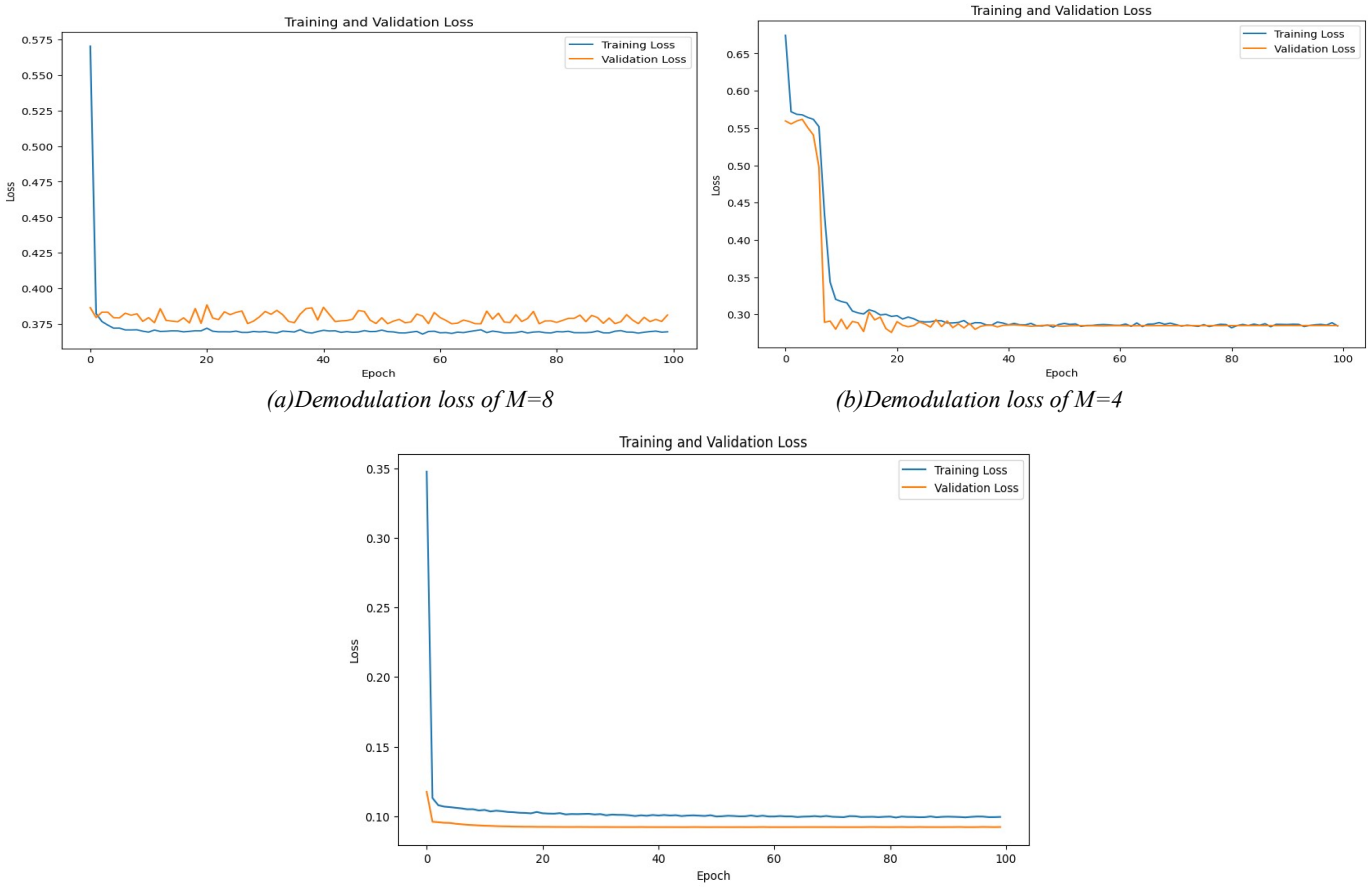

(a)Demodulation loss of M=8

(b)Demodulation loss of M=4

(c) Demodulation loss of M=2

Figure 11 The training curves depicting loss are presented in the Figure, illustrating distinct values of M, which is 8, 4, and 2.

In figure12a, 12b, and 12c present the demodulation accuracy fro M=8,4,2 respectively. The difference value comes from subtracting the ground truth from the predicted value. the ground truth is the original data in the data sets. Notably, during our iterative training of the MolCommLSTM model, there has been a consistent increase from both the training and validation accuracy scores of LSTM. After 100 epochs of careful training, the following graphs reflect some very interesting trends in the accuracy score for different values of the modulation order M. For instance, when M is set to 8, the MolCommLSTM model attains an impressive accuracy of 0.9. For M = 4, the model performs at an accuracy of 0.875. Most impressively, reducing M to 2 achieves an accuracy of 0.98 after 100 epochs.What sets this observation apart, however, is that in the context of M = 2, the MolCommLSTM model performs exceptionally, outperforming the performance achieved when M was set to either 4 or 8. Accordingly, for M = 2, the MolCommLSTM model astonishingly yields a validation accuracy as high as 0.98, against the ordinary figures of 0.9 and 0.875 obtained in the case of M = 8 and M = 4, respectively. This prominent margin reflects the drastic difference in demodulation performance of the MolCommLSTM model with M = 2 on the unseen validation dataset. A smaller value of M leads to a simpler architecture of the MolCommLSTM model with fewer parameters. Thus, such simplicity in architecture diminishes the danger of overfitting the model to the training data and provides it with an enhanced capability of generalizing well to the unseen validation data. Therefore, it goes without saying that a

significantly higher validation accuracy for M = 2 emphasizes the fact that a simpler MolCommLSTM model architecture can actually provide better performance in terms of yielding superior performance with higher accuracy on previously seen data. Therefore, the consistent increase of both training and validation accuracy scores during the training epochs testifies to the LSTM of the MolCommLSTM model on its capability to learn and capture useful demodulation features. Additionally, our results clearly point to the fact that performance peaks for the modulation order M = 2, further emphasizing the efficiency of this lower complexity model regarding demodulation accuracy on unseen data.

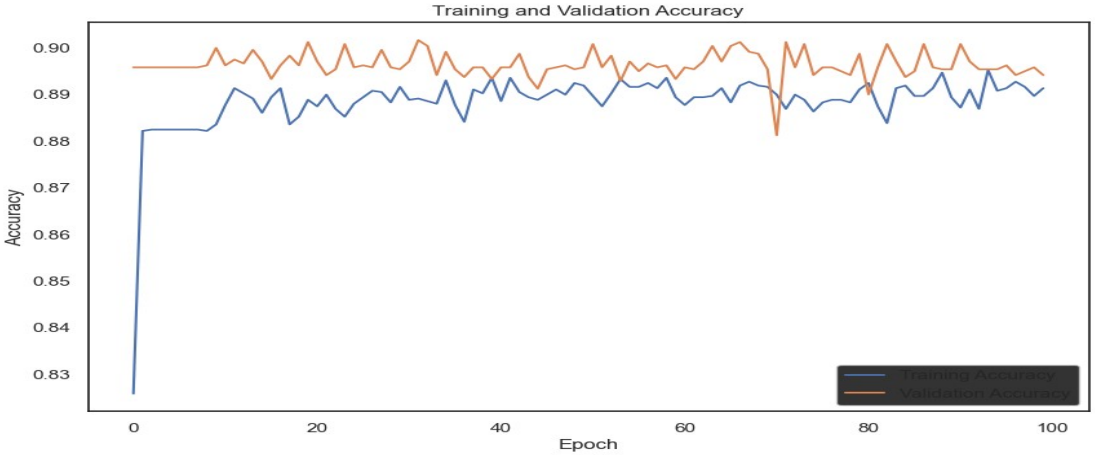

(a)Demodulation accuracy M=8

(b)Demodulation accuracy M=4

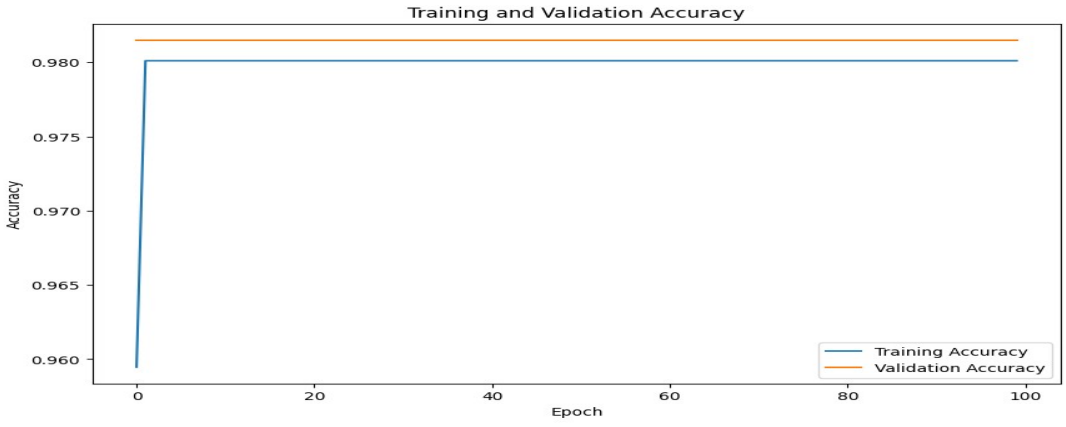

(c)Demodulation accuracy M=2

Figure 12 Demodulation accuracy curves for M=8,4,2

Journal of Theoretical and Applied Information Technology
15th May 2026. Vol.104. No.9

ISSN: 1992-8645 www.jatit.org E-ISSN: 1817-3195

5.5 Comparison Between MolCommLSTM and MLE

In our exhaustive analysis, we carried out an extensive analysis of SERs related to the use of deep LSTM in the framework of the MolCommLSTM model, compared with the MLE detection method. We present the results of our analysis in Table 2, considering the modulation order to be 8 in different distances (r = 2, 4, 6, and 8 cm) for a symbol duration, t_s = 10 sec. This analysis thus provides a much more detailed look into the performance of the MolCommLSTM model under different channel distances and for certain modulation order conditions.

Table 2 shows that when M = 8, the MolCommLSTM model outperforms MLE at all distances. For example, at 2 cm, MolCommLSTM records a much lower SER (0.096) compared to MLE (0.279). As the distance increases, this gap becomes even larger. At 8 cm, MolCommLSTM reaches an SER of (0.154), while MLE rises sharply to (0.746). Overall, the results highlight the consistent and superior performance of MolCommLSTM across all distances.

Table 2 SER comparison of MolCommLSTM and MLE at different distance when M=8.

d	2cm	4cm	6cm	8cm
MolCommLSTM	0.0960	0.1380	0.1400	0.1540
MLE	0.2794	0.2794	0.5052	0.7462

Table 3 shows that the MolCommLSTM model consistently outperforms MLE for a modulation order of M = 4 and distances of 2, 4, 6, and 8 cm at t_s= 10. MolCommLSTM achieves a SER of 0.094 at 2 cm, while MLE achieves a SER of 0.116. As the distance grows, this gap gets wider. While MLE increases to 0.530, more than double the error rate, MolCommLSTM reports a SER of 0.252 at 8 cm. These findings demonstrate the MolCommLSTM model's robust and consistent performance over a range of distances.

Table 3 SER comparison of MolCommLSTM and MLE at different distance when M=4.

d	2cm	4cm	6cm	8cm
MolCommLSTM	0.0940	0.1020	0.2440	0.2520
MLE	0.116	0.1867	0.3297	0.5304

Table 4 shows the findings for M = 2 at distances of 2, 4, 6, and 8 cm and t_s= 10. The MolCommLSTM model again demonstrates unambiguous advantage. It keeps SER values below 0.11over all distances, whereas MLE's lowest SER is 0.2206 at 4 cm. The gap gets more obvious as the distance grows. Overall, the MolCommLSTM model outperforms MLE by consistently and significantly improving SER across all modulation orders and distances investigated.

Table 4 SER comparison of MolCommLSTM and MLE at different distance when M=2.

d	2cm	4cm	6cm	8cm
MolCommLSTM	0.019	0.0311	0.0561	0.1051
MLE	0.0751	0.2206	0.3934	0.5627

Furthermore, our findings show that the MolCommLSTM model performs better for lower modulation orders, notably M = 4 and M = 2, as compared to M = 8. This discovery highlights the MolCommLSTM system model's amazing capacity to demodulate lower-order modulations with greater precision, even when working with constellations with fewer symbol points.

6. DISCUSSION

this section presents a comprehensive discussion of the proposed MolCommLSTM system by evaluation of the research objective , and highlight limitation and research issues.

The first objective of this paper was to enhance reliability of the MC system and reducing SER. The results obtained clearly demonstrate that the propose model significantly outperforms the traditional MLE-based detection over different modulation orders and transmission distances. This confirms the effectiveness of integration DL for robust detection in MC system.

The second objective was to improve ADR by adaptive modulation. The results showed that the proposed distance adaptive modulation successfully enhances data rate performance by dynamically change molecular concentration level according to the condition of the channel.

Despites these improvements, several limitation must be stated. First, the proposed system assume perfect distance estimation between transmitter and receiver ,which may be not realistic in real MC environment. Second, the model relies on simulated data, and therefore lack of validation using real biological datasets. Furthermore, while the proposed model adapts to distance variation, other factors such as mobility, noise and complex biological interaction are not fully considered. These limitations represent important open challenges the need further investigation.

Overall, the proposed MolCommLSTM model demonstrates strong potential for improving reliability and efficiency in MC systems.

7. CONCLUSIONS

In this paper, we proposed the MolCommLSTM system model, which utilizes adaptive strategy during modulation and deep LSTM for demodulation. It is considered that the MolCommLSTM system model dynamically adjusts the level of concentration based on the estimated distance between TN and RN, thereby optimizing system performance. Moreover, our approach to the system model integrates deep LSTM in order to map the received molecules to the transmitted symbols, allowing for precise and effective symbol detection. Upon evaluation of the MolCommLSTM system model, the results clearly showed that our system model significantly improved both SER and ADR, outperforming CPSK modulation schemes. The system successfully handled bias effects. The ISI within the diffusion-based channel was minimized to outperform the performance of the MLE detection method. From our perspective, the proposed work represents a promising advancement towards intelligent and adaptive MC system. However, several limitations must be acknowledged, including the reliance on accurate distance estimation, increased computational complexity, and the absence of real biological data.

Future work will focus on addressing these challenge by using real biological dataset, and enhancing interpretability to support the deployment of IoBNT applications.

REFERENCES:

[1] C. Lee, B.-H. Koo, C.-B. Chae, and R. Schober, "The internet of bionano things in blood vessels: System design and prototypes," Journal of Communications and Networks, 2023.

[2] L. Chouhan and M.-S. Alouini, "Interfacing of molecular communication system with various communication systems over internet of every nano things," IEEE Internet of Things Journal, 2023.

[3] L. Kong, L. Huang, L. Lin, Z. Zheng, Y. Li, Q. Wang, and G. Liu, "Asurvey for possible technologies of micro/nanomachines used for molecular communication within 6g application scenarios," IEEE Internet of Things Journal, 2023.

[4] Vishwamittar, P. Batra, and R. Chopra, "Molecular communication: Ananotechnological paradigm," Resonance, vol. 28, no. 1, pp. 33–53, 2023.

[5] K. Yang, D. Bi, Y. Deng, R. Zhang, M. M. U. Rahman, N. A. Ali, M. A.Imran, J. M. Jornet, Q. H. Abbasi, and A. Alomainy, "A comprehensive survey on hybrid communication in context of molecular communication and terahertz communication for body-centric nanonetworks," IEEE Transactions on Molecular, Biological and Multi-Scale Communications, vol. 6, no. 2, pp. 107–133, 2020.

[6] D. Bi, A. Almpanis, A. Noel, Y. Deng, and R. Schober, "A survey ofmolecular communication in cell biology: Establishing a new hierarchy for interdisciplinary applications," IEEE Communications Surveys & Tutorials, vol. 23, no. 3, pp. 1494–1545, 2021.

[7] I. F. Akyildiz, A. Kak, and S. Nie, "6g and beyond: The future of wireless communications systems," IEEE access, vol. 8, pp. 133 995– 134 030, 2020.

[8] A. Galal and X. Hesselbach, "Nano-networks communication architecture: Modeling and functions," Nano Communication Networks, vol. 17, pp. 45–62, 2018.

[9] T. Nakano, M. J. Moore, F. Wei, A. V. Vasilakos, and J. Shuai, "Molecular communication and networking: Opportunities and challenges," IEEE transactions on nanobioscience, vol. 11, no. 2, pp. 135–148, 2012.

[10] I. F. Akyildiz, M. Pierobon, S. Balasubramaniam, and Y. Koucheryavy,"The internet of bio-nano things," IEEE Communications Magazine, vol. 53, no. 3, pp. 32–40, 2015.

[11] B. Atakan, Molecular Communications and Nanonetworks. Springer,2016.

[12] M. S¸. Kuran, H. B. Yilmaz, I. Demirkol, N. Farsad, and A. Goldsmith,"A survey on modulation techniques in molecular communication via diffusion," IEEE Communications Surveys & Tutorials, vol. 23, no. 1, pp. 7–28, 2020.

[13] X. Wang, Z. Jia et al., "A new modulation method for diffusion molecular communication," Academic Journal of Engineering and Technology Science, vol. 4, no. 2, pp. 7–12, 2021.

[14] H. B. Yilmaz, N.-R. Kim, and C.-B. Chae, "Modulation techniquesfor molecular communication via diffusion," Modeling, Methodologies and Tools for Molecular and Nano-scale Communications: Modeling, Methodologies and Tools, pp. 99–118, 2017.

[15] N. Garralda, I. Llatser, A. Cabellos-Aparicio, E. Alarcon, and M. Pier- ´ obon, "Diffusion-

based physical channel identification in molecular nanonetworks," Nano Communication Networks, vol. 2, no. 4, pp. 196– 204, 2011.
[16] M. U. Mahfuz, D. Makrakis, and H. T. Mouftah, "A comprehensive study of sampling-based optimum signal detection in concentrationencoded molecular communication," IEEE transactions on nanobioscience, vol. 13, no. 3, pp. 208–222, 2014.
[17] S.-J. Kim, P. Singh, and S.-Y. Jung, "A machine learning-based concentration-encoded molecular communication system," Nano Communication Networks, vol. 35, p. 100433, 2023.
[18] H. Khani, "Improved detection schemes for non-coherent pulse-position modulation," Wireless Personal Communications, pp. 1–20, 2023.
[19] P. Hofmann, J. A. Cabrera, R. Bassoli, M. Reisslein, and F. H. Fitzek,"Coding in diffusion-based molecular nanonetworks: A comprehensive survey," IEEE Access, 2023.
[20] J. T. Gomez, P. Hofmann, F. H. Fitzek, and F. Dressler, "Explainability ´ of neural networks for symbol detection in molecular communication channels," IEEE Transactions on Molecular, Biological and Multi-Scale Communications, 2023.
[21] M. Kuscu and O. B. Akan, "Detection in molecular communications with ligand receptors under molecular interference," Digital Signal Processing, vol. 124, p. 103186, 2022.
[22] M. Kuscu, "Adaptive molecular communication receivers with tunable ligand-receptor interactions," arXiv preprint arXiv:2305.06481, 2023.
[23] M. Pierobon and I. F. Akyildiz, "Noise analysis in ligand-binding reception for molecular communication in nanonetworks," IEEE Transactions on Signal Processing, vol. 59, no. 9, pp. 4168–4182, 2011.
[24] M. U. Mahfuz, D. Makrakis, and H. T. Mouftah, "Strength-based optimum signal detection in concentration-encoded pulse-transmitted ook molecular communication with stochastic ligand-receptor binding," Simulation Modelling Practice and Theory, vol. 42, pp. 189–209, 2014.
[25] E. Aslan, M. E. C¸ elebi, and F. Pekergin, "Wiener and kalman detection methods for molecular communications," IEEE Transactions on NanoBioscience, vol. 21, no. 2, pp. 256–264, 2022.
[26] K. A. Alnajjar, "Low complexity detectors for mimo molecular communications under channel estimation," in 2022 International Symposium on Networks, Computers and Communications (ISNCC). IEEE, 2022, pp. 1–4.
[27] Y. Tang, F. Ji, M. Wen, Q. Wang, C.-B. Chae, and L.-L. Yang, "Probabilistic constellation shaping for molecular communications," IEEE Transactions on Communications, 2023.
[28] C. Lee, H. B. Yilmaz, C.-B. Chae, N. Farsad, and A. Goldsmith, "Machine learning based channel modeling for molecular mimo communications," in 2017 IEEE 18th international workshop on signal processing advances in wireless communications (SPAWC). IEEE, 2017, pp. 1–5.
[29] N. Farsad and A. Goldsmith, "Neural network detection of data sequences in communication systems," IEEE Transactions on Signal Processing, vol. 66, no. 21, pp. 5663–5678, 2018.
[30] X. Qian and M. Di Renzo, "Receiver design in molecular communications: An approach based on artificial neural networks," in 2018 15th international symposium on wireless communication systems (ISWCS). IEEE, 2018, pp. 1–5.
[31] T. O'shea and J. Hoydis, "An introduction to deep learning for the physical layer," IEEE Transactions on Cognitive Communications and Networking, vol. 3, no. 4, pp. 563–575, 2017.
[32] Z. Qin, H. Ye, G. Y. Li, and B.-H. F. Juang, "Deep learning in physical layer communications," IEEE Wireless Communications, vol. 26, no. 2, pp. 93–99, 2019.
[33] H. He, S. Jin, C.-K. Wen, F. Gao, G. Y. Li, and Z. Xu, "Modeldriven deep learning for physical layer communications," IEEE Wireless Communications, vol. 26, no. 5, pp. 77–83, 2019.
[34] G. H. Alshammri, W. K. Ahmed, and V. B. Lawrence, "Receiver techniques for diffusion-based molecular nano communications using an adaptive neuro-fuzzy-based multivariate polynomial approximation," IEEE Transactions on Molecular, Biological and Multi-Scale Communications, vol. 4, no. 3, pp. 140–159, 2018.
[35] S. Mohamed, J. Dong, A. Junejo et al., "Model-based: End-to-end molecular

communication system through deep reinforcement learning auto encoder," IEEE Access, vol. 7, pp. 70 279–70 286, 2019.
[36] S. Mohamed, D. Jian, L. Hongwei, and Z. Decheng, "Molecular communication via diffusion with spherical receiver & transmitter and trapezoidal container," Microprocessors and Microsystems, vol. 74, p. 103017, 2020.
[37] L. Sun and Y. Wang, "Ctbrnn: A novel deep-learning based signal sequence detector for communications systems," IEEE Signal Processing Letters, vol. 27, pp. 21–25, 2019.
[38] A. K. Shrivastava, D. Das, and R. Mahapatra, "Performance evaluation of mobile molecular communication system using neural network detector," IEEE Wireless Communications Letters, vol. 10, no. 8, pp. 1776–1779, 2021.
[39] O. D. Kose, M. C. Gursoy, M. Saraclar, A. E. Pusane, and T. Tugcu, "Machine learning-based silent entity localization using molecular diffusion," IEEE Communications Letters, vol. 24, no. 4, pp. 807–810, 2020.
[40] Y. Huang, F. Ji, Z. Wei, M. Wen, and W. Guo, "Signal detection for molecular communication: model-based vs. data-driven methods," IEEE Communications Magazine, vol. 59, no. 5, pp. 47–53, 2021.
[41] ——, "Signal detection for molecular communication: model-based vs. data-driven methods," IEEE Communications Magazine, vol. 59, no. 5, pp. 47–53, 2021.
[42] C. Bai, A. Zhu, X. Lu, Y. Zhu, and K. Wang, "Temporal convolutional network based signal detection for magnetotactic bacteria communication system," IEEE Transactions on NanoBioscience, 2023.
[43] Z. Cheng, Z. Zhang, J. Jiang, and J. Sun, "Signal detection of mobile multi-user molecular communication system using transformer-based model," in 2023 8th International Conference on Computer and Communication Systems (ICCCS). IEEE, 2023, pp. 85–90.
[44] Cheng, Z., Zhang, Z., Jin, X., Gong, W., & Chi, K. (2024). An informer-based signal sequence detector for mobile molecular communication. IEEE Communications Letters, 28(6), 1397-1401.
[45] : Xiang, C., Zhang, Y., Huang, Y., Tan, W., Chen, X., & Wen, M. (2025). Hybrid recurrent neural network for signal-dependent noise suppression in molecular communication. IEEE Transactions on Molecular, Biological, and Multi-Scale Communications.
[46] Cheng, Z., Zhang, Z., Liu, H., Jing, D., Gong, W., & Chi, K. (2025). Neural Network With Attention Mechanism for Abnormality Detection and Localization in Diffusive Molecular Communication. IEEE Transactions on NanoBioscience, 24(2), 257-267.
[47] M. U. Mahfuz, D. Makrakis, and H. T. Mouftah, "On the characterization of binary concentration-encoded molecular communication in nanonetworks," Nano Communication Networks, vol. 1, no. 4, pp. 289–300, 2010.
[48] H. Khani, "Improved detection schemes for non-coherent pulse-position modulation," Wireless Personal Communications, pp. 1–20, 2023.
[49]] L. Mucchi, A. Martinelli, S. Jayousi, S. Caputo, and M. Pierobon, "Secrecy capacity and secure distance for diffusion-based molecular communication systems," IEEE Access, vol. 7, pp. 110 687–110 697, 2019.
[50] G. Sharma, N. Pandey, A. Singh, and R. K. Mallik, "Impact of mutual influence between bob and eve on the secrecy of diffusion-based molecular timing channels," IEEE Wireless Communications Letters, vol. 11, no. 11, pp. 2255–2259, 2022.
[51] R. Mosayebi, H. Arjmandi, A. Gohari, M. Nasiri-Kenari, and U. Mitra, "Receivers for diffusion-based molecular communication: Exploiting memory and sampling rate," IEEE Journal on Selected Areas in Communications, vol. 32, no. 12, pp. 2368–2380, 2014.
[52] V. Jamali, N. Farsad, R. Schober, and A. Goldsmith, "Non-coherent multiple-symbol detection for diffusive molecular communications," in Proceedings of the 3rd ACM International Conference on Nanoscale Computing and Communication, 2016, pp. 1–7.
[53] J. Xin, C. Zhou, Y. Jiang, Q. Tang, X. Yang, and J. Zhou, "A signal recovery method for bridge monitoring system using tvfemd and encoder-decoder aided lstm," Measurement, p. 112797, 2023.